COUPLING A NEURAL NETWORK TECHNIQUE WITH CFD SIMULATIONS FOR PREDICTING 2-D ATMOSPHERIC DISPERSION ANALYZING WIND AND COMPOSITION EFFECTS

João Pedro Souza de Oliveira[3], João Victor Barbosa Alves[1,3], Ricardo de Andrade Medronho[2], Luiz Fernando Lopes Rodrigues Silva[2], João Neuenschwander Escosteguy Carneiro[4]

ABSTRACT

Computational Fluid Dynamics (CFD) defines a noteworthy methodology to carry out the numerical modeling of generic flow field problems, encompassing correlated phenomena like such as mass, momentum and heat transfer in any given geometry. Especially in gas dispersion context, such a tool presents a remarkable applicability, allowing one to perform, for example, risk assessment and consequence analysis in comprehensive analysis in areas as gas leakage and explosion scenarios risky in a comprehensive manner and consequence. Another computational technique which has gained attention in the past years is the Artificial Intelligence. An expressively widespread branch of the Artificial Intelligence paradigm consists of Machine Learning, a set of techniques of which essentially allows computer algorithms to learn from patterns in the data, successively improving the performance in predicting a given outcome. One of the most widely used types of algorithms is given by the Neural Network framework (NN), whose. The combination combined use of NN with CFD experiments has recently experienced a considerable growing growth recently in the literature academia and industry. The present work seeks to demonstrate the employment of such a coupled method in for representative problems in atmospheric dispersion representative problems. To do so, a limited set of CFD simulation results are used for developing neural networks by supervised trainings. The outcome are predictors for flow field interpolation purposes, the potential uses of which include digital twin designing, gas leakage detection optimization procedures etc. One possible way for addressing such coupling strategy, the “local approach” treats the network as a transition rule in the scope of Cellular Automata (CA), making it able to locally learn the dynamic behavior of the addressed physics. In this via, each nodal point is looked at in different time-steps; property values in the previous instant at the node and at its neighbors are taken, from which the respective fluxes are computed and serve as input to the network providing then the current node value. This method gives rise to simpler neural network architectures (fewer inputs and outputs) with closer computing relatively to the CFD calculation, but, as a downside, requires several runs of the model for each scenario in a transient fashion. Assessments have been done by predicting, first, a scalar field time evolution governed by a 1D advection-diffusion transport equation to verify the method implementation. Subsequently, species concentration distributions were sought in atmospheric dispersion cases in transient and stationary fashions modes for analyzing the capabilities regarded of the current approach’s current capability, as well as its limitations and potential to deal with the focused physics.

1. INTRODUCTION

CFD simulations have been playing a continuously more significative role in various industrial applications for flow field prediction and assessment. Gas dispersion and leakages constitute a prominent application to which such an assertion holds. Experimental measurements as well as oversimplified analytical descriptions cannot provide a detailed enough description of the addressed problems. Numerical modelling via CFD, on the other hand, is capable to provide sufficiently accurate predictions at engineering level, offer a framework that allow to compute approximations for real case gas dispersion scenarios.

As a downside, the solutions returned by a CFD calculation derive from a physical domain discretization. Dense computational grids designed to represent large or complex geometries may impose some restrictions in the analysis to be performed due to CPU time limitations and processing capacity. With the growing diffusion of machine learning resources, like Artificial Neural Networks (ANN), several engineering

1 D.Sc, Candidate, School of Chemical - Federal University of Rio de Janeiro
2 Ph.D, Professor of School of Chemical - Federal University of Rio de Janeiro
3 M.Sc, R&D Engineer – ISDB FLOWTECH
4 Dr.-Ing., Managing Partner – ISDB FLOWTECH

modellings bottlenecks have been addressed by formulating data-driven models, whose potential encompasses the construction of either hybrid strategies or concentrated parameters correlations (black-box approach).

A combined treatment CFD-ANN can be structured in distinct ways, serving the same or different purposes. A possible goal in utilizing this method consists of predicting field variables by a surrogate data-driven model after applying a computational learning technique employing the gathered CFD results. Hence, one may seek for interpolation or even extrapolation ends when building such a coupled approach.

In order to compute distributed flow properties in a coupled CFD-ANN scope, two paths can be followed in terms of the architecture scale. Particularly, the target focused by the learning procedure distinguishes these paths. A global approach deals with the whole flow field domain, receiving discretization points and boundary/initial conditions directly as inputs. By processing these inputs through a typically complex deep learning architecture owing to high data dimensionality, distributions flow properties can be provided. An example of this path is given in the study carried by [1]. Conversely, a "local" framework looks at individual discretized elements (equivalent or not to the prescribed CFD mesh) –treated in fact as system's unities –, in which local and instantaneous information are taken and processed to evaluate next instant variables' local values.

The regarded local modelling can be obtained in the context of Cellular Automata (CA). A scan looking at each computational cell (an automaton) take respective the tracked variables' values corresponding to the current time-step and from its neighbors. By applying a transition rule, one updates the cell state to the next time-steps. A coupling between both CA and ANN techniques can be achieved by using the last as a transition rule [2].

The present work aims to develop a surrogate model by structuring a data-driven strategy in the sense of CA-ANN coupling, sohence a "local" treatment, to perform interpolations or extrapolations once gas dispersions CFD simulation results datasets are provided

2. DESCRIPTION

Three cases with increasing level of complexity were selected in order to assess the methodology. First, an extremely simple reference problem was addressed to verify the general consistency of the concept and its implementation: a 1D transient advection-diffusion scalar equation. Next, the analysis focused on 2D gas dispersion scenarios, which are the focus of the present study. Specifically, a transient puff and cloud displacement in a free atmospheric dispersion defined the first 2D case, and a continuously feed steady state 2D plume, the second one.

For all cases, the local treatment succeeded following the schematic procedure illustrated in Fig. 1. That is, in a scan for each time-step, one accesses the variables determining the current state of a given computational node. To get the updated local state, a trained ANN processes the input data, which comprises neighbors current time states besides those of the scanned node. In the stationary case, a similar structure is considered. However, the desired steady state of every node results from a processing of local coordinates directly during the scan, as well as the case's boundary condition varied throughout the training dataset.

To perform the model building, codes were written in Python 3.8.11 using the Machine Learning package TensorFlow 2.6.0.

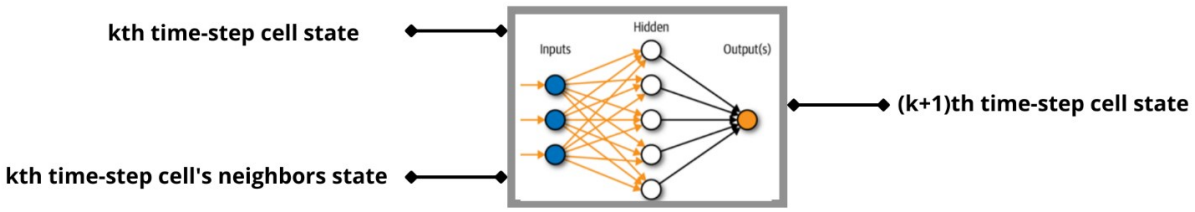

Fig.1 *– Local approach scheme.*

2.1 1D TRANSIENT ADVECTION-DIFFUSION SCALAR TRANSPORT EQUATION

The governing equation of the 1D scalar transport by advection and diffusion processes in the transient regime can be written as:

$$\frac{\partial \varphi}{\partial t} + c\frac{\partial \varphi}{\partial x} + d\frac{\partial^2 \varphi}{\partial x^2} = 0 \quad (1)$$

where φ denotes a generic scalar field, and c and d represent advective (as follows, a constant velocity distribution is imposed) and diffusive coefficients, respectively.

Tab. 1 summarizes *the boundary* and initial conditions, inputs, outputs and ANN architecture main hyperparameters. The problem consists of solving the time advancement of the referred scalar subjected to Dirichlet boundary conditions and starting from a null distribution. The 1D domain (disposed in x = [0,1] interval) was discretized in five-nodes *only,* with the purpose of verifying the implementation.

Tab.1 – 1D problem specifications

Boundary conditions	$\boldsymbol{\varphi(t, x = 1) = 0, \varphi(0, x) = 0}$ $\boldsymbol{\varphi(t, x = 0)} = \{1.5,2.0,2.5,3.0,0.5,3.5,4.0,4.5\}$
Density and diffusivity	$\boldsymbol{\rho = 1, \Gamma = 0.1}$
Features	$\varphi_0, \frac{\partial \varphi_0}{\partial x}, \frac{\partial^2 \varphi_0}{\partial x^2}, \varphi_{0,w}, \varphi_{0,e}$
Labels	φ^{curr}
Hidden layers	3 (10-10-10)
Normalization	$\varphi^{norm} = \frac{\varphi - \overline{\varphi}}{\sigma_\varphi}$
Loss function	$LogCosh = log\left(\frac{exp(\varphi) + exp(-\varphi)}{2}\right)$

As reported in Tab. 1, the initial distribution and right boundary are null. The dataset composition comes from varying the left boundary condition. φ^{curr} and φ_0 denote current and past time-step scalar values, respectively. $\overline{\varphi}$ symbolizes the scalar mean and σ_φ, the scalar standard deviation. The presented derivatives were calculated in the Finite Volume Method (FVM) framework, using the cell neighbors' values.

The procedure provided in Fig. 2 depicts the steps needed for applying the combined strategy addressed.

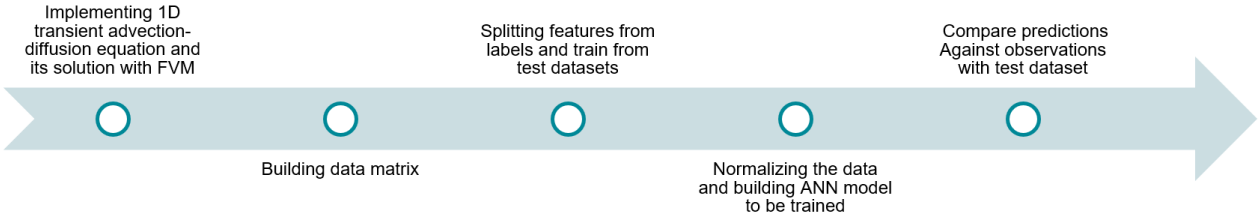

Fig.2 *– Steps for succeeding with the coupled strategy.*

2.2 2D Puff and Cloud Displacement in Atmospheric Gas Dispersion

The second scenario refers to a gas dispersion given by a short time release of methane (a puff) and its development as a cloud being carried by a forward pure air flow. The proposal here is to assess the model's ability for handling a transient behavior related to the regarded physics. Tab. 2 provides the case specifications.

The second scenario refers to a gas dispersion given by a short time release of methane (a puff) and its development as a cloud being carried by a forward pure air flow. The proposal here is to assess the model's ability for handling a transient behavior related to the regarded physics. Tab. 2 provides the case specifications.

The problem setup starts from the generation of a dataset for ANN training by performing CFD simulations of a 3m x 2m rectangular domain, whose left edge, around its center, contains a 10cm methane (4% CH4 + air mixture) injection hole while air enters through its remaining extension at 3 m/s. Following [2], the similar case definition and boundary conditions were applied at top and bottom boundaries (symmetry) and at the right edge (pressure-outlet). Fig. 3 illustrates a schematic representation of the discretized computational domain created in ICEM CFD and simulated using the CFD solver Fluent, both for Ansys v2020R1 package.

Simulations were run in order to assess the molar concentration distribution at different time-steps. The temporal lapse employed in the simulations does not need to be equal to the one used in the data-driven approach. The ANN, once satisfactorily trained, is expected to extract implicitly the time correlation amongst the dataset built by combining cells scan for different instants. In special, concentration distributions correspondent to the time interval of 15.6s to 19.2s were selected, divided in subintervals of 0.4s. Test dataset, not presented during the training epochs, represent 20% of all cells' values, being used for prediction performance checking. A single time window, that is, considering only the last time-step for composing the network input, was design in this assessment.

Tab.2 – 2D puff and cloud displacement specifications

Boundary conditions	Pure air inlet: 3 m/s (velocity inlet) Injection hole: 3 m/s and 4% of CH_4 + air (velocity inlet) Top and bottom contours: symmetry Outlet: P_{static} = 0 Pa (pressure-outlet)
Features	$C_{i,0}, \frac{\partial C_{i,0}}{\partial x}, \frac{\partial C_{i,0}}{\partial y}, C_{i,0,w}, C_{i,0,e}, C_{i,0,s}, C_{i,0,n}$
Labels	C_i^{curr}
Hidden layers	4 (25-75-75-25)
Normalization	$\varphi^{norm} = \frac{\varphi - \overline{\varphi}}{\sigma_\varphi}$
Loss function	$MAE = \sum_{i=0}^{N} \lvert \varphi_{true} - \varphi_{pred} \rvert$

2.3 2D Steady State Plume

The third case investigated was given by a stationary plume developed through a free atmospheric dispersion in consequence of a continuous injection of a contaminant (methane). The simulated system consisted of a 5m x 2m rectangular domain, the discretization of which resulted in a 6300 quadrilateral cells computational grid. The imposed boundary conditions follow in Fig. 4 and comprises the methane admission through a 10cm hole placed around the left edge's center and opening boundaries at top, bottom and right contours, the first two assigned with pressure inlet condition while the last was set with pressure outlet condition.

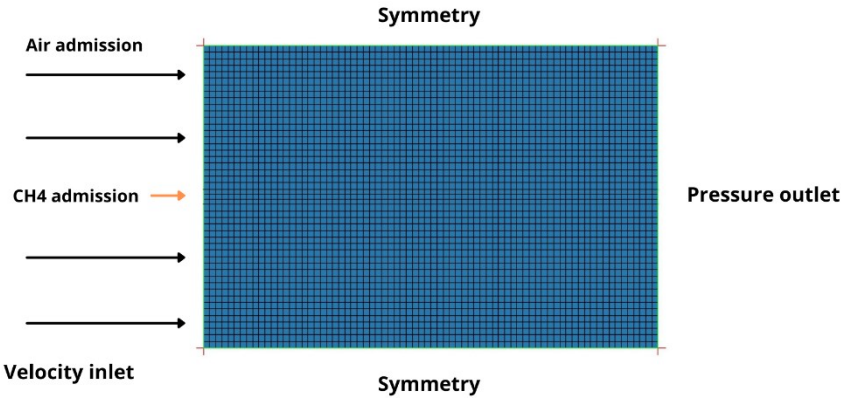

Fig.3 *– 2D puff and cloud displacement 3600 quadrilateral cells mesh and boundary conditions.*

In Tab.3, specifications related to network settings as well as boundary conditions are given. It is worthy to stress the fact that the database building for train and test occurred by considering different flow rates in the simulations runs for the methane leakage, specifically in the velocities range indicated for the inlet contour.

In contrast with the transient cases previously described, an explicit geometry dependency takes place when using the regarded approach in a stationary fashion. The local scan that follows accesses each cell's X and Y coordinates values. The ANN developed transition rule is expected not to return a proper state update in a time advancement sense, but the corresponding local distributions of properties relevant to the concerned physics (velocities and concentrations), which complete the uniquely addressed steady state. Besides spatial location, the cells evaluated at different conditions receive the respective inlet velocity as an input to particularize their associated field.

It is important to note that the specific geometric inputs were formulated in terms of distances to the boundaries. Proceeding this way, one expects to alleviate the direct spatial discretization dependency since the network may learn to identify how the different boundary condition influences a given region of the domain as a function of proximity.

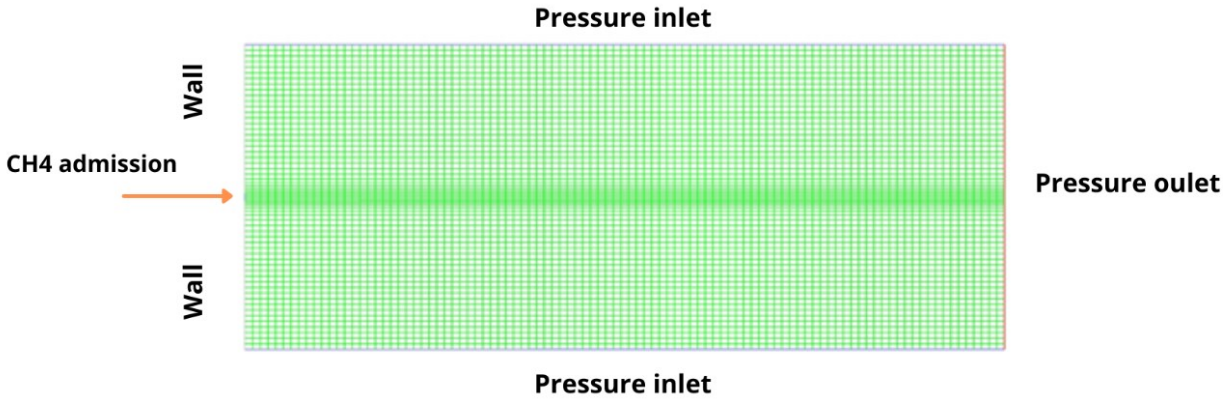

Fig.4 *– 2D steady state plume computational grid.*

Tab.4 – 2D steady state plume specifications.

Boundary conditions	Injection hole: {0.1, 0.2, …, 0.9} (velocity inlet) Top and bottom contours: P_{total} = 0 Pa (pressure inlet) Outlet: P_{static} = 0 Pa (pressure-outlet)
Features	$D_{left}, D_{right}, D_{top}, D_{bottom}, V_{in}$
Labels	$C_i^{SS}, V_{x,i}, V_{y,i}$

Hidden layers	7 (75-75-75-75-75-75-75)
Normalization	$\varphi^{norm} = \frac{\varphi - \overline{\varphi}}{\sigma_{\varphi}}$
Loss function	$MAE = \sum_{i=0}^{N} \lvert \varphi_{true} - \varphi_{pred} \rvert$

2.4 2D Transient Jet

The fourth case considered was the transient analogous of the previous one, then featuring a plume in development as an outcome of a continuous injection of a contaminant (methane). It resembles a transient jet. The same conditions remained in the current scenario with respect to computational domain shape and discretization, as well numerical simulations settings. The exception is that its run occurred in the transient regime.

It is noteworthy to mention an important difference concerning the database building. For the sake of exploration of the methodology's extension, the dataset included a single contaminant injection velocity (specifically, 0.6 m/s). The addressed data variability referred to the local molar concentration field time at different timesteps. The resulted ANN featured a similar architecture as described in Tab.4 with regards to hyperparameters. A distinction took place for input and output variables. Tab.5 summarizes the model's setup.

Tab.5 – 2D transient jet specifications.

Boundary conditions	Injection hole: 0.6 (velocity inlet) Top and bottom contours: P_{total} = 0 Pa (pressure inlet) Outlet: P_{static} = 0 Pa (pressure-outlet)
Features	$C_{i,0,w}, C_{i,0,e}, C_{i,0,s}, C_{i,0,n}, C_{i,0}, C_{i,1}, C_{i,2}, C_{i,3}$
Labels	${C_i}^t$(First architecture) and $\{{C_i}^t, {C_i}^{t+1}\}$ (Second architecture)
Hidden layers	5 (30-30-30-30-30)
Normalization	$\varphi^{norm} = \frac{\varphi - \varphi_{min}}{\varphi_{max} - \varphi_{min}}$
Loss function	$MAE = \sum_{i=0}^{N} \lvert \varphi_{true} - \varphi_{pred} \rvert$

After a brief exploratory analysis, a 4 time-step window was taken, which means that local concentrations related to the 4 previous time-step defined the model's features. Besides the proper cell's state, concentrations of the neighboring cells at left, right, up and down directions for the immediate previous instant also formed the input variables set. Two architectures were assessed: one predicting the current local field state and other returning also the first future time-step state.

The dataset was organized into cell states corresponding to concentration field taken at 5 time-step sets, the first four combined to provide through the network the predicted current states. Train and test subsets resulted from a partition between these groups.

2.5 2D Steady State Upward Wind

The fifth case consisted of a stationary flow field developed in a contaminant gas dispersion resulted from a forward leak subjected to an upward constant velocity wind. The computational domain and its discretization follow in Fig.5, as well the boundary condition's locations, whose specifications is summarized in Tab.6 along with neural network's hyperparameters and variables.

It is valid to stress details concerning to database building. Differently to the procedure applied in the previous steady case, the coordinates X and Y were cut off as input features during cells scan performed in the regarded approach. Poor results have taken place in the first trials, a fact that motivates changing the input variables in analogy to the transient cases, i.e., a concentration field associated to a prescribed condition whose expected role is to be a kind of initialization.

To do so, distinct pairs of conditions composed the dataset, being differentiated by inlet velocities assigned to contaminant leakage and the wind. Variations in these parameters should produce the same sought steady state field independently of the fed field. It is like the transient framework, in which database elements are discriminated in terms of the correspondent instant, but the dependence with the input field is expected to be mitigated by randomizing the conditions. For example, the same input field giving different results by changing only the variations in inlet velocities.

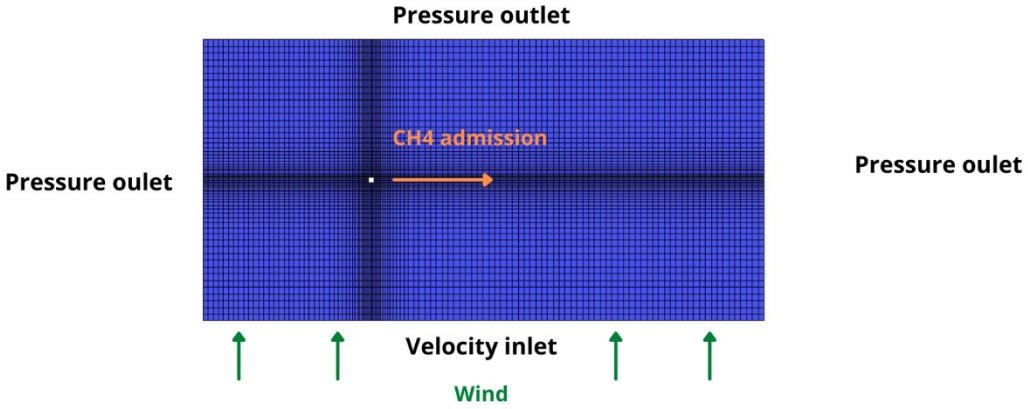

Fig.5 *– 2D steady upward wind 7425 quadrilateral cells computational grid.*

Tab.6 – 2D upward wind case specifications.

Boundary conditions	Injection hole: {0.25, 0.5, 1.0, 1.0, 2.0, 3.0, 4.0, 5.0, 6.0} m/s (velocity inlet) Left, top and right contours: P_{static} = 0 Pa (pressure outlet) Bottom: {0.1, 0.2, 0.3, 0.4, 0.5, 0.6, 0.7, 0.8, 0.9, 1.0} m/s (velocity-inlet)
Features	$C_{i,prescribed}, \Delta V_{leak}^{in}, \Delta V_{wind}^{in}$
Labels	${C_i}^t$(First architecture) and $\{{C_i}^t, {C_i}^{t+1}\}$ (Second architecture)
Hidden layers	3 (20-20-20)
Normalization	$\varphi^{norm} = \frac{\varphi - \varphi_{min}}{\varphi_{max} - \varphi_{min}}$

Loss function	$MAE = \sum_{i=0}^{N} \lvert \varphi_{true} - \varphi_{pred} \rvert$

3. RESULTS AND DISCUSSION

In this section, the considered study cases allowed to assess the performance of the coupled CFD-ANN local strategy treated.

3.1 1D Transient Advection-Diffusion Scalar Transport Equation

Training results for the generated neural network follow in Fig.5. One may observe that the fitting procedure led to a very good representativity of the data distribution, which can be observed through the very. Moreover, a comparison plot between the true scalar values and model predictions indicates that the current network architecture has a good predictive capacity, since a test subset containing 20% of the raw dataset has never been used during the learning process.

In order to ensure the trained data-driven model's ability to accurately produce scalar distributions and its time evolution by means of a local framework (i.e., performing a scan through individual nodes), an interpolation scenario was investigated. Specifically, the field time advancement related to a left boundary condition of φ(x=0,t)=2.3 (not included in original dataset) was taken. Fig.6 provides a plot comparing the FVM solutions and NN predictions at different time-steps.

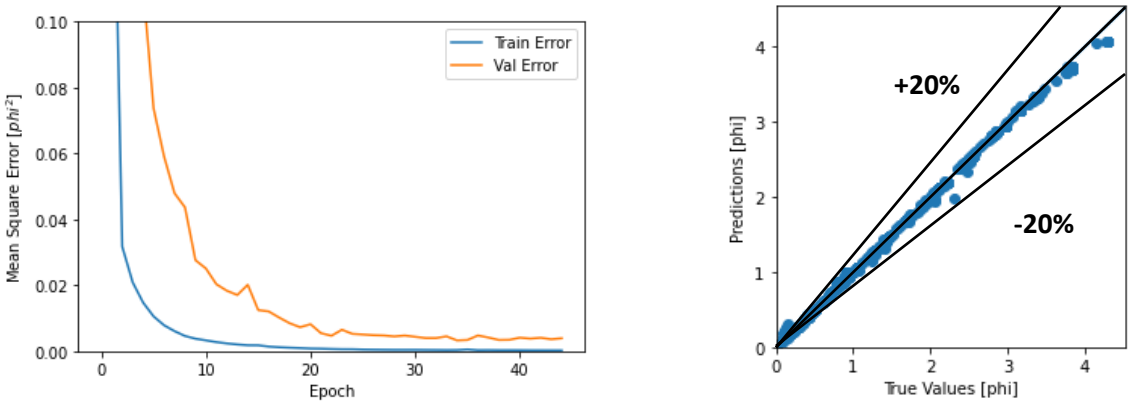

***Fig.6** – 1D transient advection-diffusion case training reports: (left) mean squared error evolution during training – validation subset error considered for early stopping technique use; (right) observations versus predictions in test dataset.*

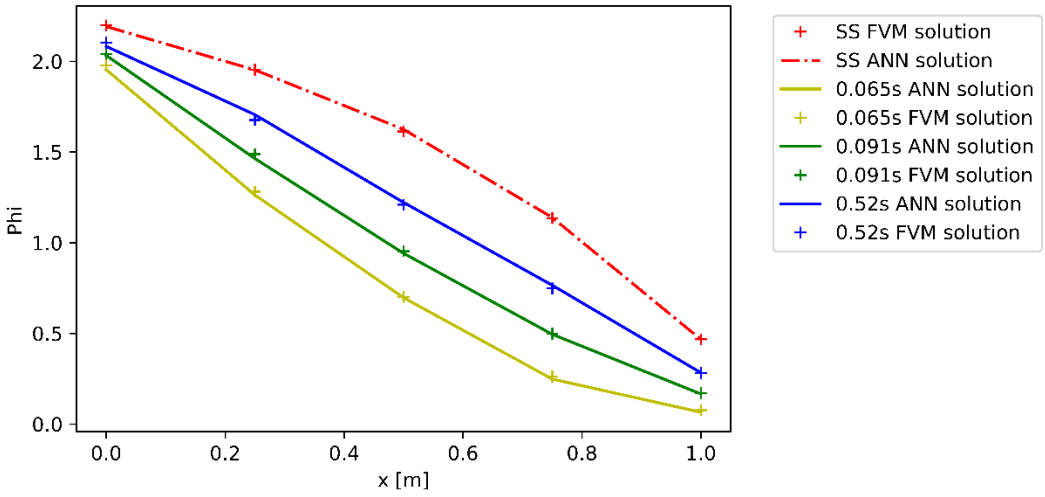

Fig.7 *– 1D transient advection-diffusion scalar field time evolution: comparison of FVM and ANN results for different time-steps up to steady-state.*

The matching plots illustrated in Fig.6 constitutes an important indicative of the consistency of the methodology. The model seemed to have a learning capacity to address the physical phenomena investigated (advection and diffusion). Following the initial investigation with a simple 1D problem, it is important to assess multi-dimensional cases and how different boundary conditions and presence of eventual mass sources influence the results, which will be presented in the following sections.

3.2 2D Puff and Cloud Displacement in Atmospheric Gas Dispersion

The ANN training for the puff and cloud displacement study case also showed a satisfactorily performance. As depicted in Fig7, low levels of the "Mean Squared Error" (MSE) were reached. The expressive agreement for predictions of the test subset revealed that the adjusted data-driven model presents, again, an acceptable predictive capacity.

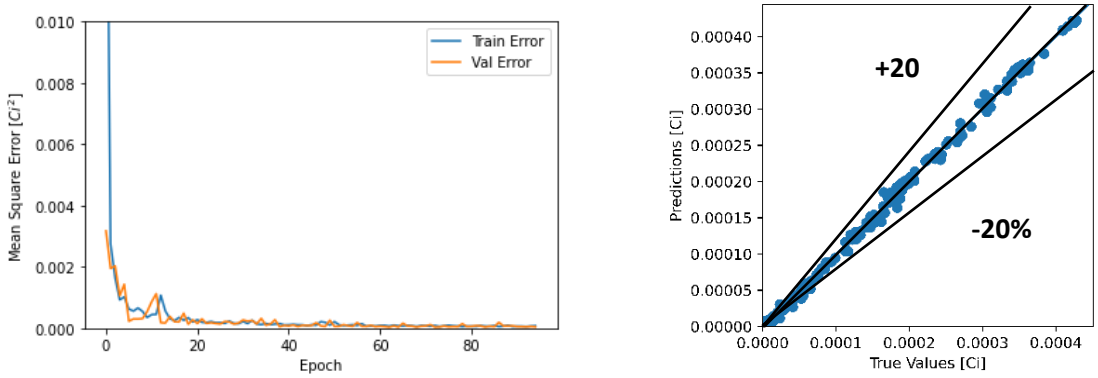

Fig.8 *– 2D puff and cloud displacement case training reports: (left) mean squared error evolution during training – validation subset error considered for early stopping technique use; (right) observations versus predictions in test dataset.*

The ANN structure is based on the local approach. That is, the inference returned by such a model acts recursively on the domain discretization cells. In this context, it is imperative to verify capacity of the network to represent cells connectivity, capturing a consistent and accurate concentration field time evolution. Hence, the prediction of molar concentration of methane correspondent to one time-step was addressed in what follows. In particular, the comparison took the one time-step transition between instants 15.6s and 16s.

In Fig.9, the cloud position associated to the initial time considered is provided. It follows in Fig.10 representations of the resulted distribution after the time transition generated by the constructed data-driven model and related to the CFD simulation results dataset.

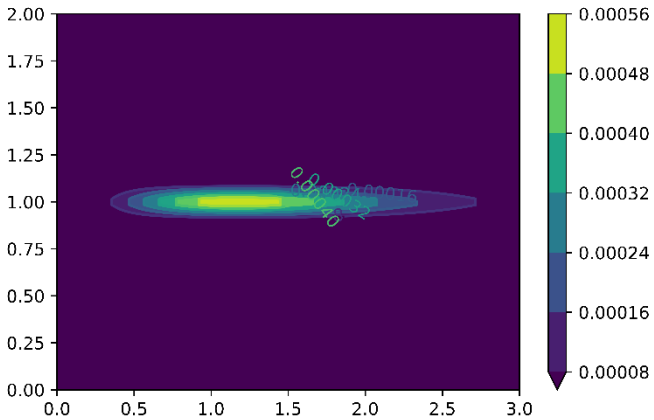

Fig.9 *– 2D puff and cloud displacement case molar concentration field for the instant of 15.6s.*

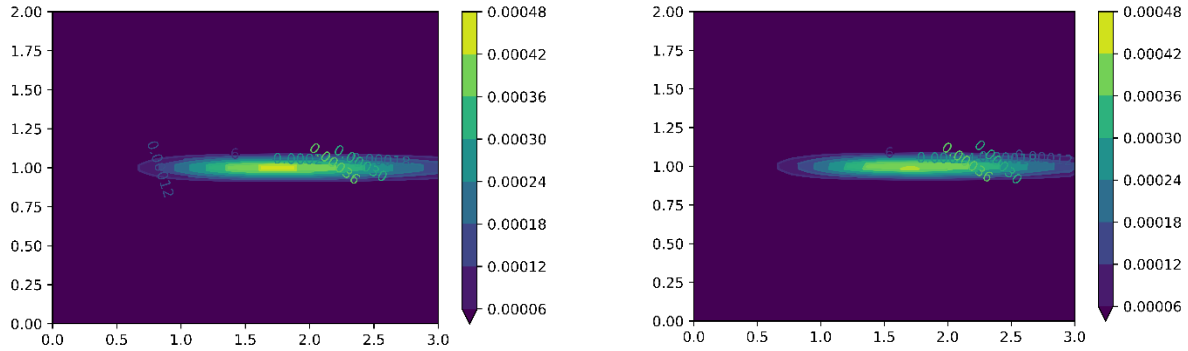

Fig.10 *– 2D puff and cloud displacement case molar concentration field for the instant of 16s: (left) reference CFD data; (right) ANN prediction.*

One may note that a considerable agreement resulted from the comparison accomplished. Although promoting the cells state update in a recursive fashion, taking each one at once, a coherent total distribution could be obtained. Nevertheless, a single time-step window established in the training step limited the network in extracting the time correlation between inputs and outputs for an arbitrary time advancement to be reproduced.

[3] has identified two distinct inference modes for an ANN designed for transient flow field predictions: cascading and non-cascading. Ideally, the aim of such a coupled approach is to start from an initial field and return its time evolution, feeding the network with previous time-steps solutions to compute the current time one: the cascade mode. Though prediction errors tend to accumulate, this could produce deprecated solutions after fewer time-steps. Thus, it is still a challenge passing from individual time-steps predictions by a data-driven surrogate model to a full-time evolution framework trained with CFD simulations.

3.3 2D Steady State Plume

Two ANNs were built in the 2D stationary plume formation with the architecture specifications listed in Tab.4. One has as its target the molar concentration field while the other predicts the two components of velocity distribution. The training performance for these networks follow in Fig.10 and Fig.11, being given in terms of accuracy evolution for train and validation subsets and comparison between predicted and true values for the test subset.

A similar behavior could be observed as that described in the previous study case. An oscillatory profile in the ANN error is observed during the parameter adjustment procedure. However, sufficiently small losses were reached in a couple of epochs, indicating the achievement of a reasonable fitting. Furthermore, the comparison involving observations in the test subset and their respective model predictions showed an acceptable predictive capacity. These appointments are valid for both networks training assessments, although the oscillatory pattern was significantly more pronounced in the inference of velocity components.

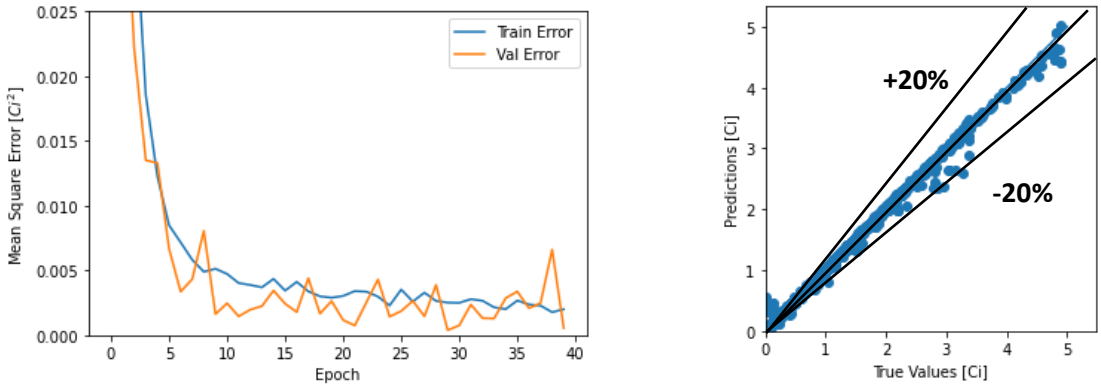

Fig.11 *– 2D steady state plume case training reports for prediction of molar concentration: (left) mean squared error evolution during training – validation subset error considered for early stopping technique use; (right) observations versus predictions in test dataset.*

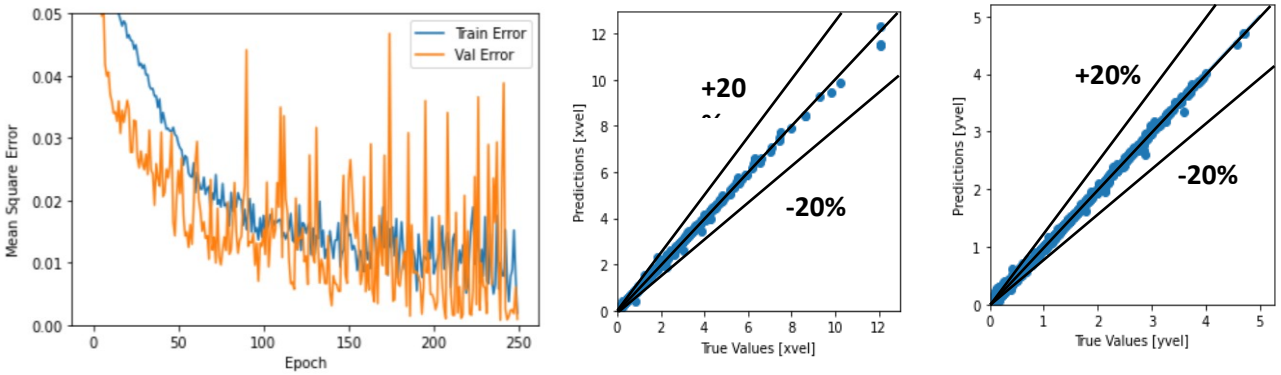

Fig.12 *– 2D steady state plume case training reports for prediction of velocity field components: (left) mean squared error evolution during training – validation subset error considered for early stopping technique use; (middle) observation versus predictions in test subset for x axis velocity component; (right) observations versus predictions in test subset for y axis velocity component.*

Analogously to other cases analyzed, it is fundamental to verify the reconstruction of the target fields with the obtained model. Fig.12, Fig.13 and Fig.14 depict predictions corresponding to an extrapolation scenario. The train and test dataset encompasses steady flow fields for different inlet velocities to the methane leakage in the range starting in 0.1m/s up to 0.9m/s, as one may see in Tab.4. These plots refer to a methane admission at 1.0m/s.

It must be emphasized that the agreement provided by the coupled CFD-ANN approach for this study case constitute an important indication of the local treatment potential. Originally designed to transient calculations as proposed in [2], the same framework seems to be applicable in a stationary fashion, by changing consistently the input variables. An explicit geometric dependency take place, which could be softened by expressing it in terms of distances to boundaries, as well as a direct imposition of the main conditions defining the diverse scenarios, i.e., the entrance flow rate (or inlet velocity) information.

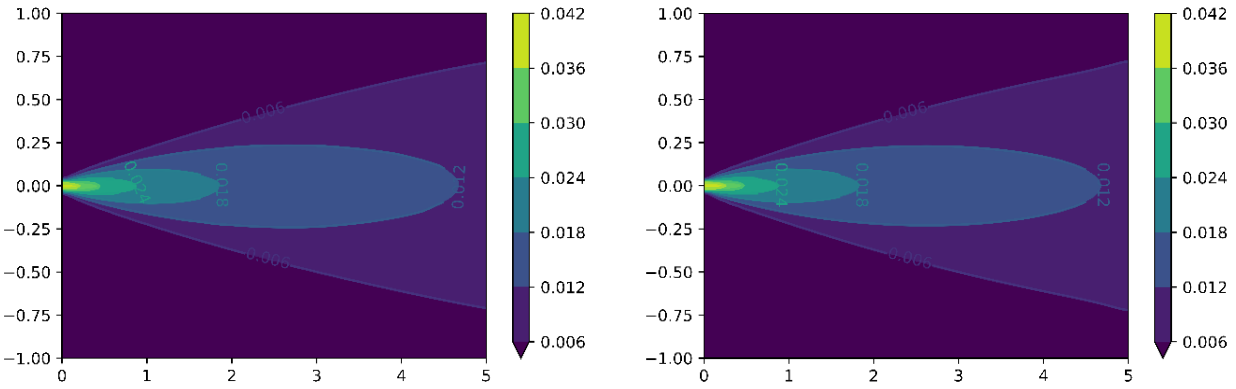

Fig.13 *– 2D steady state plume case molar concentration field prediction for: (left) reference CFD data; (right) ANN prediction.*

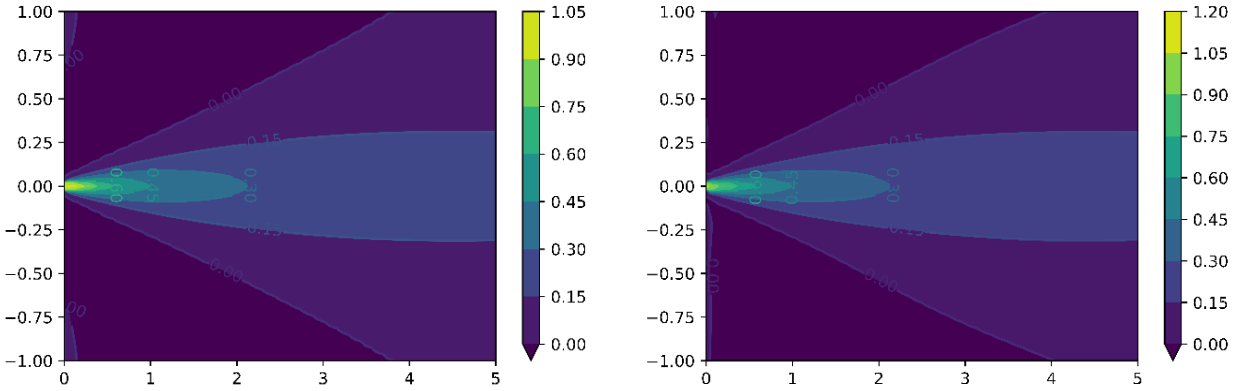

Fig.14 *– 2D steady state plume case x axis velocity component field prediction for: (left) reference CFD data; (right) ANN prediction.*

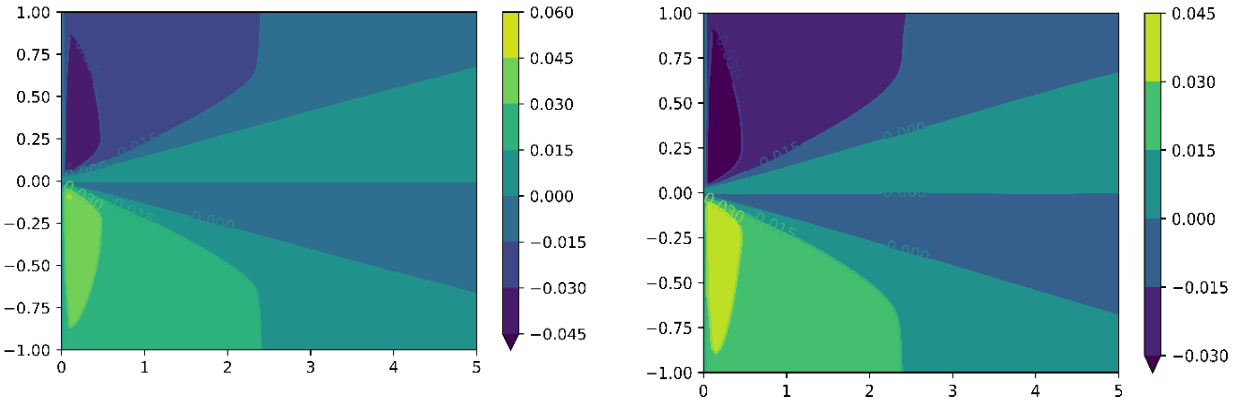

Fig.15 *– 2D steady state plume case y axis velocity component field prediction for: (left) reference CFD data; (right) ANN prediction.*

3.4 Transient Jet

Two architectures were built in the 2D transient jet formation presenting the specifications listed in Tab.4. Their difference is the number of future time-steps predicted at once. Fig.16 reports their training performance, as well as predictability for train and validation subsets. Moreover, a comparison is exhibited between predicted and true values for the test subset.

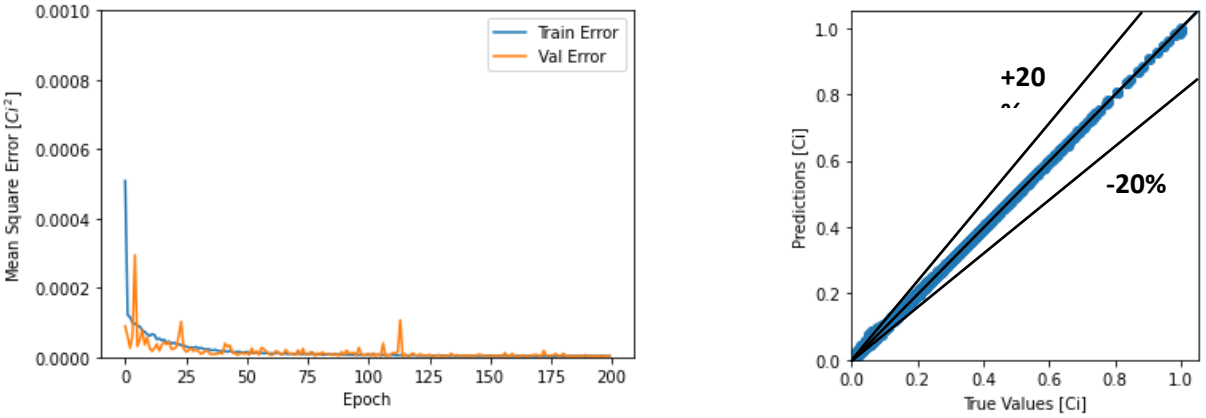

Fig.16 *– 2D transient jet case training reports: (left) mean squared error evolution during training – validation subset error considered for early stopping technique use; (right) observations versus predictions in test dataset.*

In Fig.17, it follows the same performance reports for the second model structured, encompassing two plots of predicted versus observed values that refer to each generated output (current and first future time-step cell states).

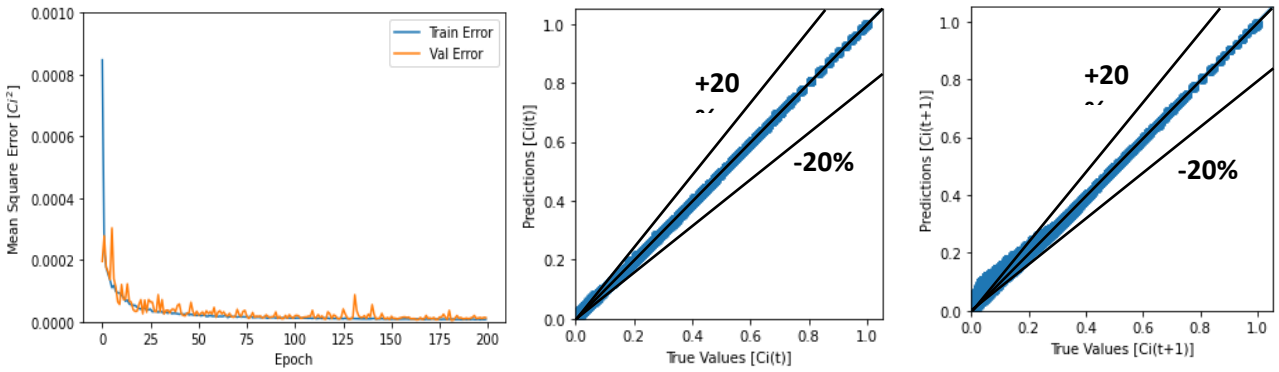

Fig.17 *– 2D transient jet case training reports for prediction of velocity field components: (left) mean squared error evolution during training – validation subset error considered for early stopping technique use; (middle) observation versus predictions in test subset for current molar concentration prediction; (right) observations versus predictions in test subset for next time-step molar concentration prediction.*

As it can be observed, a reasonable fitting resulted for the regarded architectures in terms of both training performance (by achieving sufficiently low mean squared errors levels for train and validation subsets) and test subset assessment, in which the returned agreements between predictions and observations point to a generalization capability.

Once built and trained, one must apply such models for field computation in order to visualize the time evolution of the plume. In Fig.18, it follows the prediction and its correspondent database element first time-step range (using from the first to the fourth to predict the fifth). Next, Fig.19 portrays the range constituting the test subset (13-16 time-steps for evaluating the seventeenth one). A further assessment was accomplished by extending the whole time-step window to a series of unseen concentration fields (17-20 time-steps for evaluating the twenty-first one).

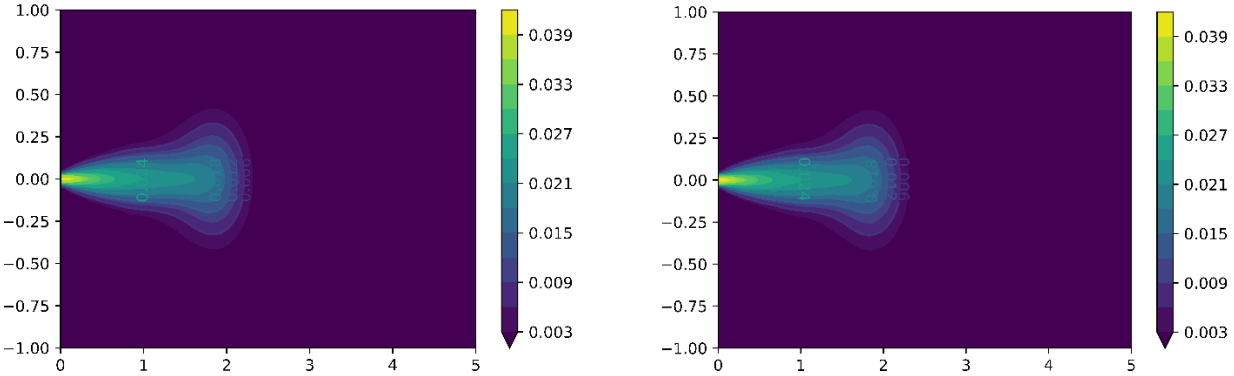

Fig.18 *– 2D transient jet case methane molar concentration field prediction at the fifth time-step (25s) for: (left) reference CFD data; (right) ANN prediction.*

As it can be seen, acceptable agreement is obtained the comparisons considered. This behavior indicates that the followed data-driven approach has a potential for extracting time evolution features. The expected pattern occurred for the time sequence after the range presented in the train dataset, which is worth to highlight. Nevertheless, a limitation arises from the restricted prediction only for the next time-step. Also, the time window width as well as time-step size constitute relevant factors to deeper understand, the impacts of which should be assessed for stating the methodology's real potential.

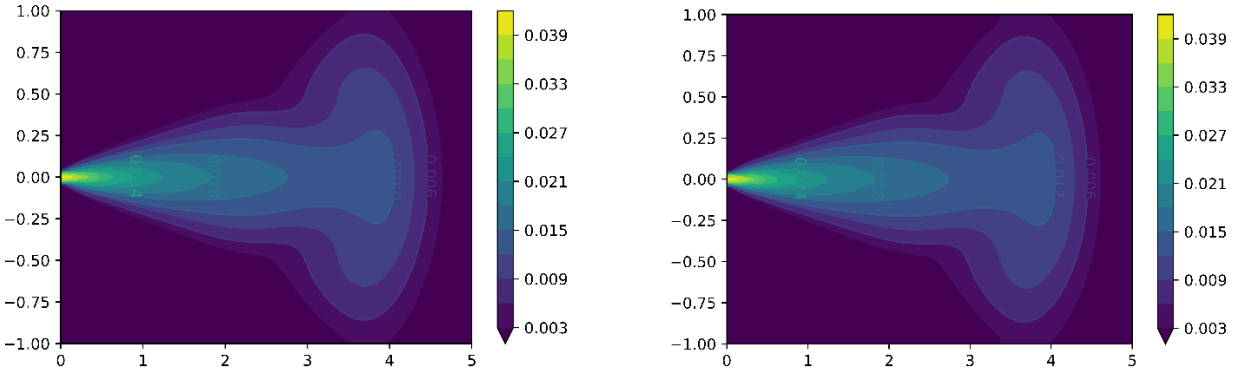

Fig.19 *– 2D transient jet case methane molar concentration field prediction at the seventeenth time-step (42.5s) for: (left) reference CFD data; (right) ANN prediction.*

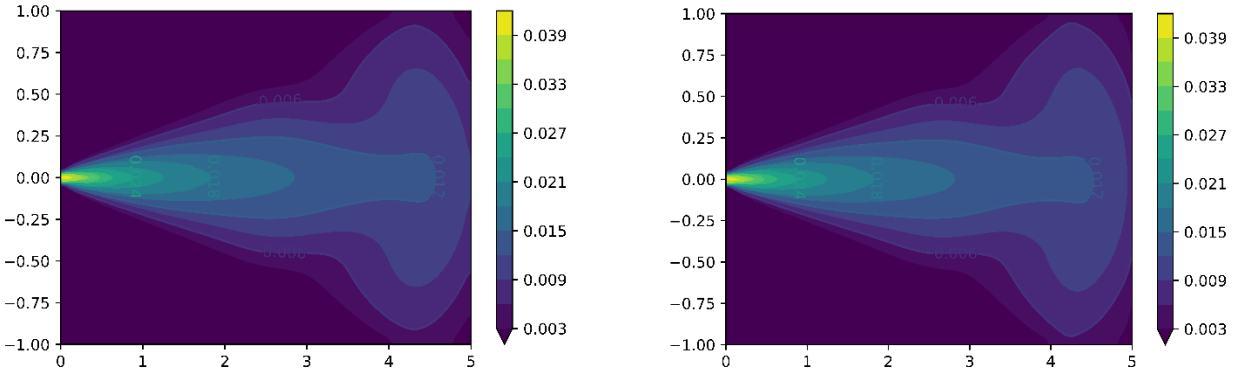

Fig.20 *– 2D transient jet case methane molar concentration field prediction at the seventeenth time-step (52.5s) for: (left) reference CFD data; (right) ANN prediction.*

In order to address the issue above, a modification was investigated by generating the second model, which can predict subsequent time-steps. The reports regarding its application included two time-step ranges. Fig.20 and Fig. 21 portray results observed and calculated regarding the range (3-8) using the first four fields and returning the fifth and sixth ones, a case belonging to the train subset. Fig.22 and Fig.23 provide the same comparison for time-steps ranging from the thirteenth to the eighteenth, in which the last two correspond to fields in future instants.

A local limitation resulted for one of the unseen concentration fields in the train procedure. The first time-step field was reproduced satisfactorily, whereas the subsequent showed a distortion in the jet's front zone. Such deviation may lead to error accumulation when extending the predictions to further instants. A possible modification to improve the performance may come from increasing previous time-steps fed to the network as input. This solution, however, would imply an increase in CFD data demand.

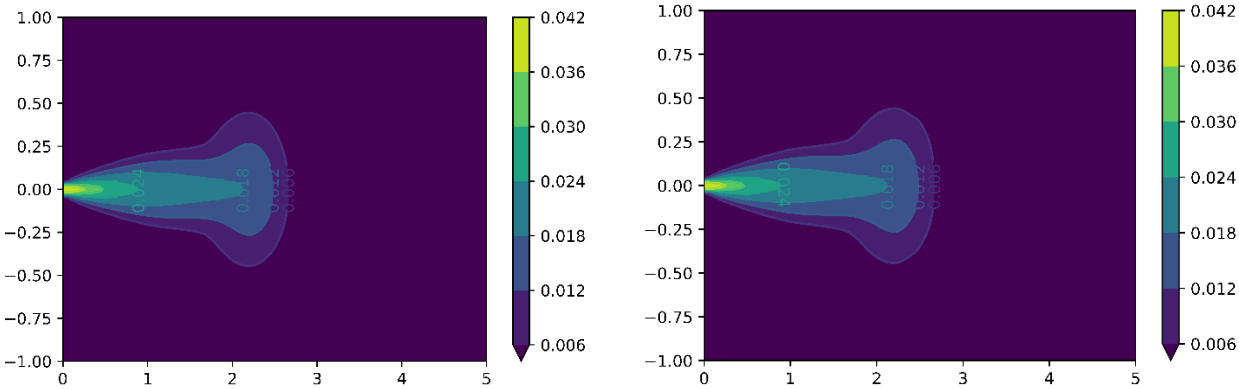

Fig.21 *– 2D transient jet case methane molar concentration field prediction at the seventh time-step (17.5s) for: (left) reference CFD data; (right) ANN prediction.*

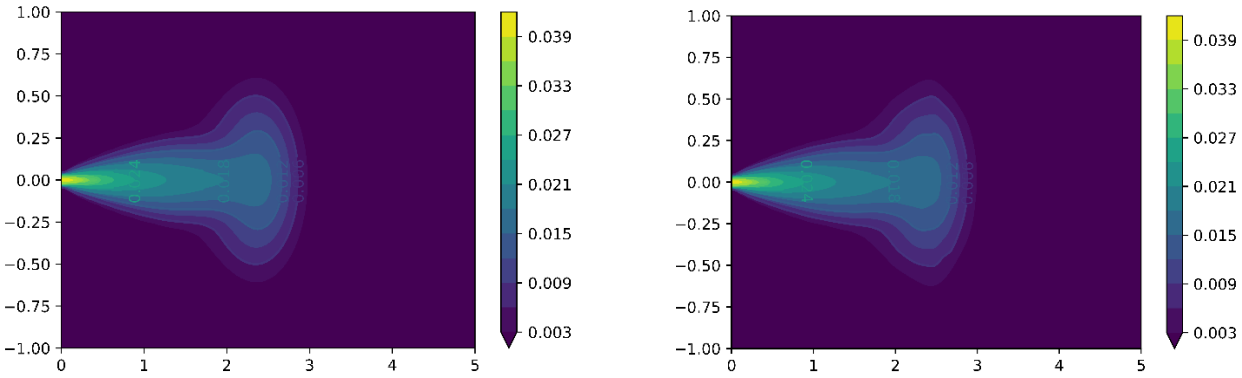

Fig.22 *– 2D transient jet case methane molar concentration field prediction at the eighth time-step (20.0s) for: (left) reference CFD data; (right) ANN prediction.*

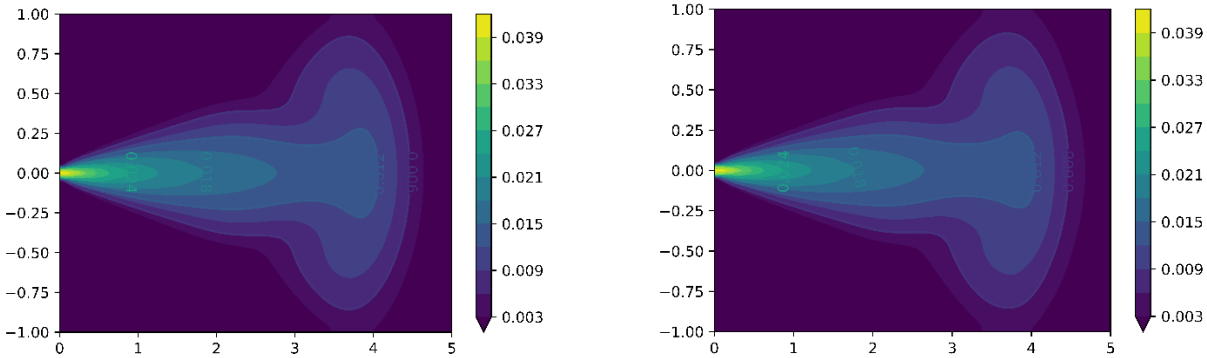

Fig.23 *– 2D transient jet case methane molar concentration field prediction at the seventeenth time-step (42.5s) for: (left) reference CFD data; (right) ANN prediction.*

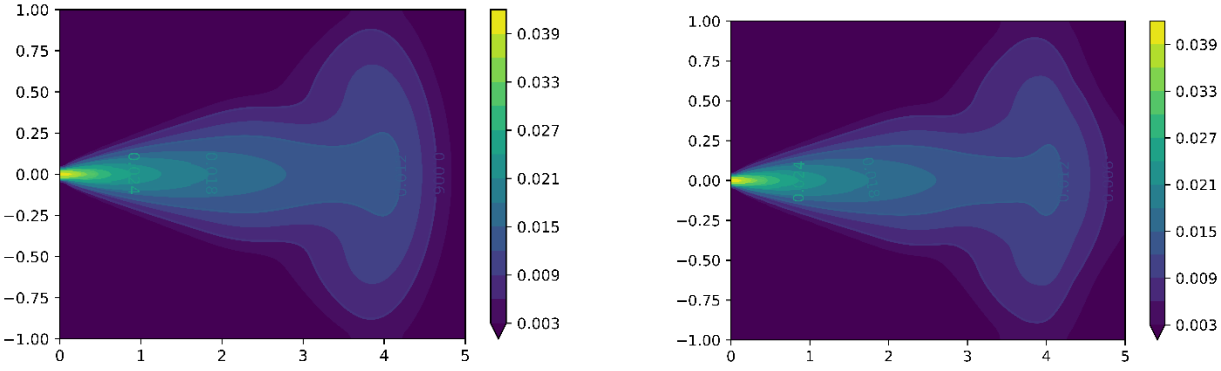

Fig.24 *– 2D transient jet case methane molar concentration field prediction at the eighteenth time-step (45.0s) for: (left) reference CFD data; (right) ANN prediction.*

3.5 Upward Wind

The ANN training performance follows in Fig.25, being assessed by mean squared error decay tracking. Its generalization capability was inferred from the comparison using the test subset, an analysis reported in Fig.25. Low levels of the chosen accuracy metric were reached, indicating an expressive representation of

fields contained in train subset. The majority of test data could be captured by the model. Nonetheless, a significative spread resulted, meaning a restriction in the generalization capacity.

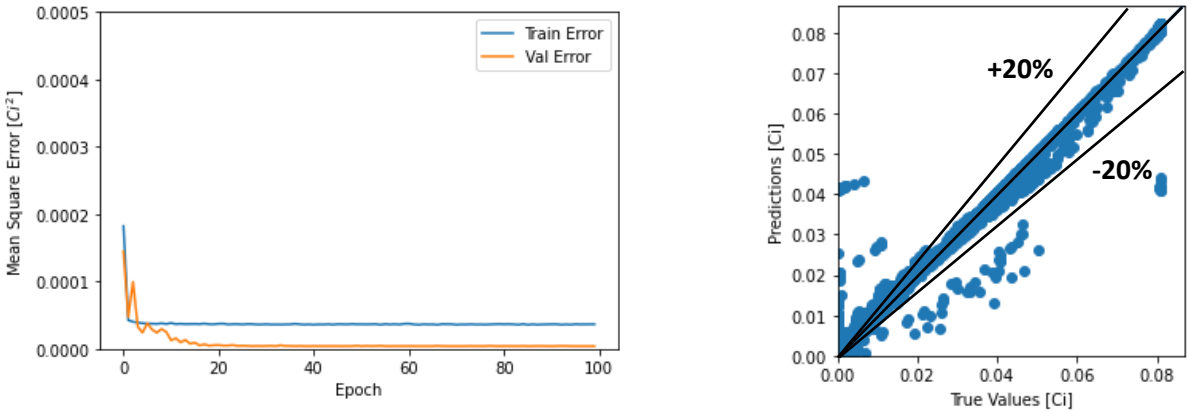

Fig.25 *– 2D upward wind case training reports: (left) mean squared error evolution during training – validation subset error considered for early stopping technique use; (right) observations versus predictions in test dataset.*

The test subset comprised an arbitrarily selected set of concentration fields pairs discriminated by velocities of upward wind and contaminant leakage injection. Following the local strategy of accessing individual cells for state update, the current case set a more challenging problem for the proposed modelling. This assertion derived from addressing sensible concentrations patterns varied with the magnitude imposed to the two inlet conditions. A different strategy was used in relation to the 2D steady state plume case, consisting of receiving a concentration field correspondent to a given condition and, by means of the variations in the inlet velocities, the model is expected to provide the correspondent steady state field.

One needs to visualize network's predictions. Hence, in Fig.26, it follows the result returned for a condition of the train subset. Specifically, it reads the distribution correspondent to a leakage velocity of 0.5m/s and an upward wind at 0.1m/s to calculate the one for a leakage velocity of 2.0m/s; the proper inputs to the model consisted of velocities variations of 1.5m/s and 0m/s, besides the local state of each cell accessed. A reasonable reproduction could be observed.

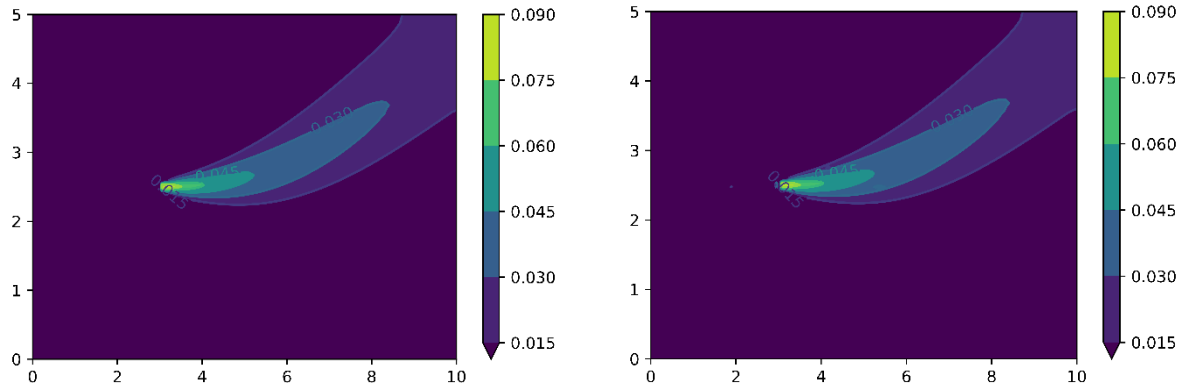

Fig.26 *– 2D steady upward wind case methane molar concentration field prediction at leakage velocity of 2.0 m/s and upward wind velocity of 0.1 m/s for: (left) reference CFD data; (right) ANN prediction.*

A similar plot (Fig.27) was made for a test subset flow condition. A case with leakage velocity changing from 3.0 m/s (input) to 6.0 m/s (output) and wind velocity passing from 0.2 m/s to 0.7 m/s. One may realize an acceptable concordance, the absolute error distribution of their following in Fig.28. Noteworthily, by combining different input steady fields for computing others, also steady, with several variations in the inlet

velocities, it was attempted to reduce the influence of the concentration field fed to the network, accessing its nodes individually, in other to predict the desired steady condition. In other words, it was intended to establish the prescribed concentration field constituting an input as a initialization to the model that is expected to provide the interpolation sought.

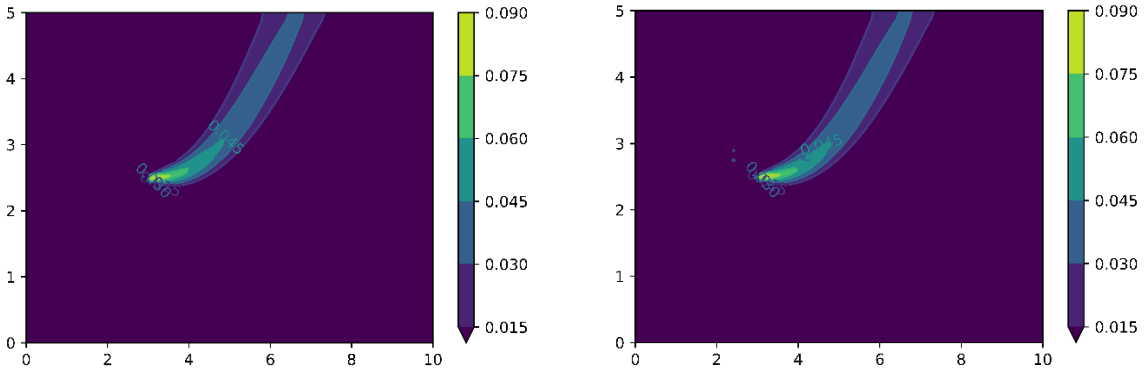

***Fig.27** – 2D steady upward wind case methane molar concentration field prediction at leakage velocity of 6.0 m/s and upward wind velocity of 0.7 m/s for: (left) reference CFD data; (right) ANN prediction.*

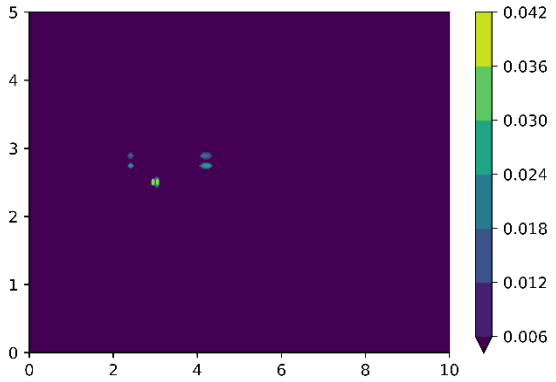

***Fig.28** – 2D steady upward wind case methane molar concentration field absolute error prediction at leakage velocity of 6.0 m/s and upward wind velocity of 0.7 m/s.*

4. CONCLUSION

A coupled CFD-ANN approach was investigated in order to demonstrate its potential for dealing with gas dispersion and leakages predictions by combining a database building from reduced amounts of CFD results with the employment of computational learning algorithms, which would return a surrogate modelling serving primarily for interpolation purposes. Moreover, a local treatment was followed, whose main feature consists of recursively accessing the nodes that form the analysis discretization in either modes training or inference.

The first case study allowed to address the capability of the methodology to capture the principal transport processes involved in the target physics, advection and diffusion, in the absence of other complexities, which may be included progressively in future studies. For this simple problem, excellent agreement resulted between the reference FVM solution and the data-driven model for the prediction of the scalar field time advancement in an interpolation scenario. It indicates the implementation consistency, essential to proceed further assessments.

Passing to 2D case studies, problems in transient and stationary regimes were considered. In the first, the time evolution of a contaminant cloud was assessed, moving in a free atmospheric dispersion after the occurrence of a puff (instantaneous release). A considerable matching resulted in the comparison of the prediction and the CFD reference data for molar concentration field at one time-step transition. Nevertheless, as an important task that has remained, one needs to modify the ANN structure or training routine seeking to improve the time correlation extraction by the model.

The second 2D problem consisted of predicting a steady state methane plume in a free field. The observations thus made from the analysis performed in this scenario indicated that the local treatment originally developed for a transient regime presents a potential to be applied in a stationary fashion. The input variables fed for ANN processing were changed to distances to boundaries and inlet velocity of the correspondent case. The two networks constructed with equal architectures demonstrated to be able to accomplish an inference of molar concentration and the two velocity components in an extrapolation case.

An analysis was performed by applying the regarded approach to model the same 2D plume case but in a transient fashion. So, the variables selected as inputs come back to be previous instants local concentrations. In particular, the analysis employed a 4 time-step window, i.e., the network processes the 4 previous instants fields to calculate the current one. Another model was also built using the same architecture that the previous with exception of predicting two next time-steps field instead of one. Promising outcomes were obtained concerning to predict satisfactorily the remain flow field time series. The extension of the prediction range, however, showed a slight limitation in the accuracy of the farther instant field; an observation that need to be deeper investigated for determining its real impact.

The last case consisted of a steady state problem in which the wind effect was preliminarily assessed: an imposed upward wind at constant velocity changing the direction of a plume coming from a methane leakage forward. Different combinations of prescribed inlet velocities applied to wind and contaminant injection composed the CFD simulation results database. A distinct strategy relatively to the former steady case allowed achieving reasonable predictions, showing a potential for further development of the coupled CFD-ANN approach.

Further features bringing different levels complexities to the modeled flow field must be accounted for in future work. Additionally, a special concern exists with respect to ensuring overall conservation of the predicted physical quantities. Machine learning tools like neural networks and deep learning networks seems to constitute a potential way to conciliate more detailed time-consuming numerical simulations with the data-intensive statistical and optimization methods by interpolation or extrapolation. Physics-informed data-driven approaches are considered a possible way forward.

5. REFERENCES:

[1] SONG D., LEE K., PHARK C., SEUNGHO J. “Spatiotemporal and layout-adaptive prediction of leak gas dispersion by encoding-prediction neural network”. *Process Safety and Environmental Protection*. 2021. 151:365-372.

[2] LAURET P., HEYMES F., APRIN L., JOHANNET A. “Atmospheric dispersion modeling using Artificial Neural Network based cellular automata”. *Environmental Modelling and Software*, Elsevier, 2016, 85, pp.56-69

[3] ANSARI A, BOOSARI SSH, MOHAGHEGH SD (2020) “Successful Implementation of Artificial Intelligence and Machine Learning in Multiphase Flow Smart Proxy Modeling:Two Case Studies of Gas-Liquid and Gas-Solid CFD Models”. *J Pet Environ Biotechnol*. 11:401. doi: 10.35248/2157-7463.20.11.401